

## COARSENING KINETICS IN Al ALLOY CAST THROUGH RAPID SLURRY FORMATION (RSF) PROCESS

Robin Gupta<sup>1)\*</sup>, Ashok Sharma<sup>1)</sup>, Upendar Pandel<sup>1)</sup>, Lorenz Ratke<sup>2)</sup>

<sup>1)</sup>Department of Metallurgical and Materials Engineering, Malaviya National Inst. of Technology Jaipur-302017, India

<sup>2)</sup>Department of Aerogels, DLR German Aerospace Centre, Inst. of Mater. Research, Linder Hohe-51147, Cologne, Germany

Received: 18.11.2016

Accepted: 22.02.2017

\*Corresponding author: Email: rbn Gupta@gmail.com, Tel.: +919982592546, Department of Metallurgical and Materials Engineering, Malaviya National Institute of Technology Jaipur, Rajasthan, India

### Abstract

In the present investigation, the rate of coarsening kinetics was discussed on conventional diffusional Lifshitz, Slyozov and Wagner (LSW) theory, coarsening by convective mass flow and coalescence by stirring speed. The rate of coarsening kinetics was found to be faster than predicted by diffusional LSW theory, but slower than predicted by the convective mass flow. The effect of flow pattern with baffles in a crucible at different holding time was also examined. The results showed that use of baffles produced fine and more globular primary  $\alpha$ -Al phase when compared to sample processed without baffles having the same holding time.

**Keywords:** Rapid slurry formation, enthalpy exchange material (EEM), stirring speed, holding time, microstructure, baffle

### 1 Introduction

The RSF process depends on enthalpy exchange between two alloy systems having different enthalpies levels but with same composition [1]. The solid metal used as a stirrer and known as enthalpy exchange material (EEM). The EEM dissolved in the melt to give a pre-decided solid fraction. In coarsening kinetics, small particles grow by reducing solid/liquid interface free energy. The reduction in interfacial energy is the driving force for the coarsening kinetics and known as Ostwald ripening. The mechanism for Ostwald ripening was given by the Lifshitz, Slyozov, and Wagner and known as LSW theory. Based on LSW theory as holding time increased the average grain size of primary  $\alpha$ -Al phase also increased [2].

Many investigators [3-6] studied the coarsening kinetics for different alloys. Birol [3] studied the coarsening kinetics of A357 alloy cast through cooling slope process. The observation showed that coalescence dominated in the early stages of isothermal holding, while Ostwald ripening appeared to be the principal mechanism in the later stages. Lashkari et al. [4] studied the coarsening of the semi-solid A356 alloy at pouring temperature of 595°C. Their observation showed that as the holding time increased at that point coarsening of primary  $\alpha$ -Al phase mainly occurred due to the two mechanisms, Ostwald ripening and coalescence. Atkinson et al. [5] studied the microstructural coarsening of recrystallisation and partial melting (RAP) 2014 and cooling slope (CS) of 2014 (Al-4Cu-0.8Si) and 201 (Al-4Cu-0.05Si) alloy. The coarsening rate for CS

201 was higher than the RAP 2014 or CS 2014. Haghdadati et al. [6] observed the coarsening rate constant of A356 alloy cast through the accumulative back extrusion (ABE) process. The experimental value of coarsening rate constant obtained in ABE process was higher than the value of coarsening rate constant in another process (SIMA, ultrasonic vibrations and angular oscillations).

In the present investigation to understand about the coarsening kinetics in RSF process various mechanisms e.g. LSW theory, convective mass flow, and coalescence by shear flow were discussed. In LSW theory, the theoretically and experimental value of coarsening rate constant was calculated. A study of the coarsening kinetics without and with the use of baffle was also carried out. The baffles were used to investigate the flow pattern during metal casting. Baffles impede rotational flow and diminished unwanted flow and due to this, the samples processed with baffles comprised the fine and more globular primary  $\alpha$ -Al phase than the samples processed without the use of baffles.

## 2 Experimental material(s) and methods

A schematic diagram of the RSF process was shown in **Fig. 1**. The EEM cylindrical in shape (5 cm diameter and 7.3 cm long) and 0.373 kg in weight were taken to prepare the solid fraction about 30wt.% of the melt. The EEM was cast on a steel stirrer rod. The shape of the rod did not result in any shearing effect upon dissolution of the submerged EEM. The rod with EEM was joined to a device having rotation speed up to 1800 rpm. 1.35 kg of A356 alloy (composition given in **Table 1**) was melted in a crucible at 700°C.

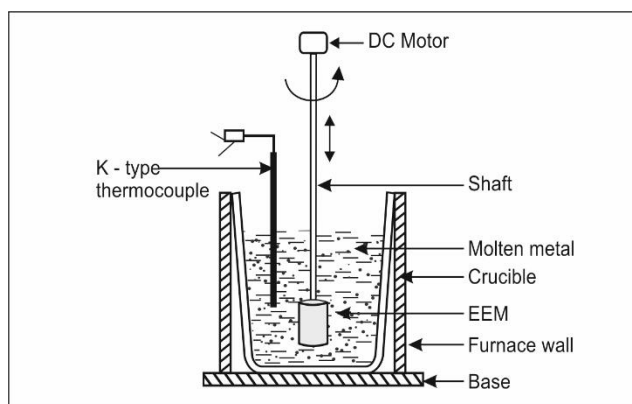


**Fig. 1** Schematic diagram of different stage involved in the RSF process

**Table 1** Chemical composition of A356 alloy [wt.%]

A356	Si	Mg	Cu	Fe	Mn	Al
wt%	6.97	0.34	0.03	0.02	0.10	92.54

The EEM was slowly lowered into the melt and stirring started with the preset rotation speed of 400 rpm. During mixing, the slurry was formed rapidly within 30 seconds and kept at 597°C. The slurry was quenched into the water after achieving the desired conditions. Similar experiments were performed for higher rotational speeds 600, 800, 1000, and 1200rpm. Coarsening kinetics was studied for the holding time 3min, 5min, 10min, and 15min followed by quenching in water.

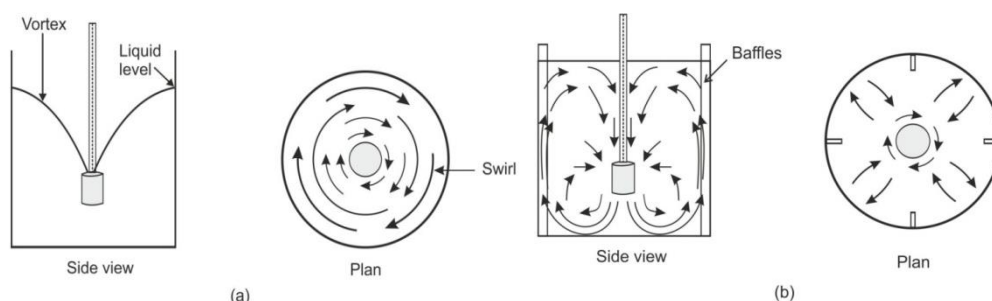
Microstructure investigations with standard metallographic procedures were carried out. The samples were polished using emery paper of grade 0/0, 1/0, 2/0, 3/0, 4/0 and alumina of grit 600, 800, and 1000. After polishing, etching with Keller's reagent was also carried out. ASTM International test standards E 112-12 used for measuring the average grain size [7].

### 3 Result and Discussions

#### 3.1 Flow pattern

The type of flow pattern in a crucible comprised a decisive role in mixing, and it depends on the size and geometry of vessel, type of stirrer, and the nature of the fluids. The stirrer created a flow pattern in the system causing the liquid to circulate through the crucible and return eventually to the stirrer. The stirrer exhibited three main tasks to perform; (i) disperse solid into a liquid, (ii) prevent agglomeration of the solid droplets in any part of the vessel and (iii) to provide convective heat transfer to the cooling surface [8].

The velocity of the fluid in the crucible illustrated three components radial, tangential and longitudinal. In general, the radial and tangential components were in the horizontal plane, and the longitudinal component was in vertical. The radial and longitudinal components were useful and provided the necessary flow for the mixing action. The tangential flow attained a circular path around the shaft and created a vortex on the surface of the liquid as shown in **Fig. 2(a)**.

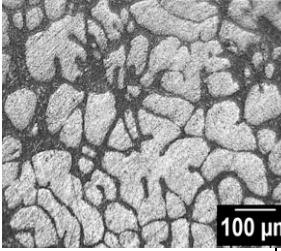
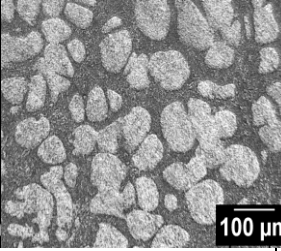
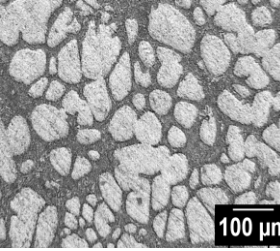
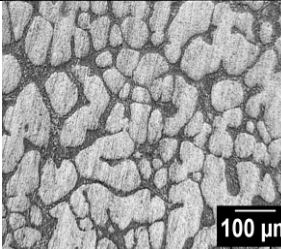
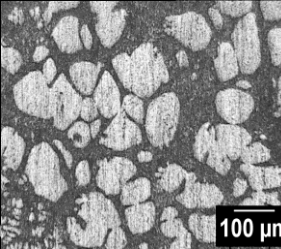
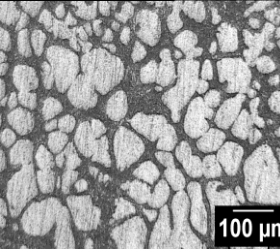
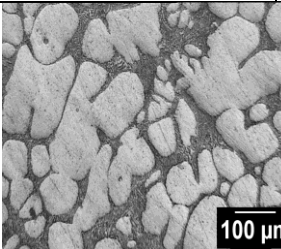
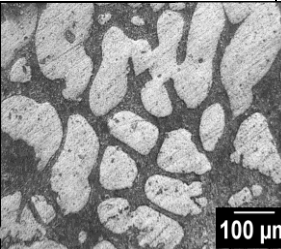
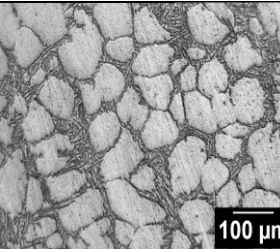
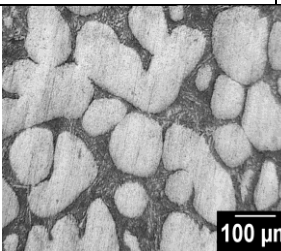
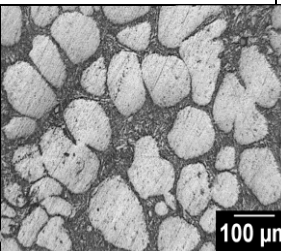
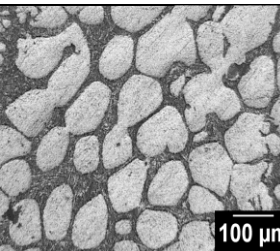
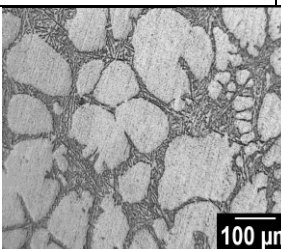
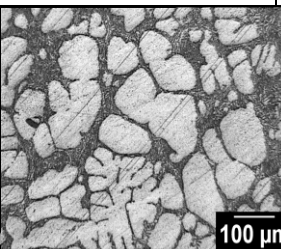
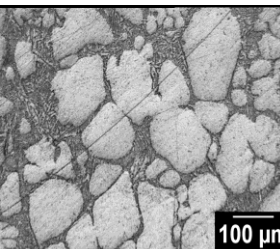


**Fig. 2** Typical flow pattern in (a) un baffled, (b) baffled crucible

Without baffle, crucible produced swirling motion and due to this vortex formation occurred which lacks adequate mixing. Vortex formation also leads to air aspiration which is not desirable. These phenomena can be avoided by using baffles along the crucible walls. Typically four baffles were used having equal width and placed at 90° intervals as shown in **Fig. 2(b)**. The purpose of baffled to suppress vortex formation and convert swirling motion into a preferred flow pattern so that proper mixing may take place [9]. Baffles impeded rotational flow without interfering with the radial or longitudinal flow.

#### 3.2 Coarsening kinetics: without the use of baffles

Coarsening is a diffusive-competitive multi-particle growth problem. The curvature of particles controls the diffusion of solute and thus the dissolution and growth kinetics of the particles. When the matrix exhibited precipitates of various sizes, this inhomogeneity drives the solute from smaller to larger precipitates. This is due to Gibbs Thompson effect [10] in which the solubility of a particle is directly proportional to its curvature. **Fig. 3** showed the microstructures for A356 alloy and structure evolution during semi-solid state at 597°C. Dendrites in as-cast condition changed into globular morphology when stirring was carried out at the different stirring speed.

Time (min.)	Stirring speed (rpm)		
	400	600	800
0			
3			
5			
10			
15			

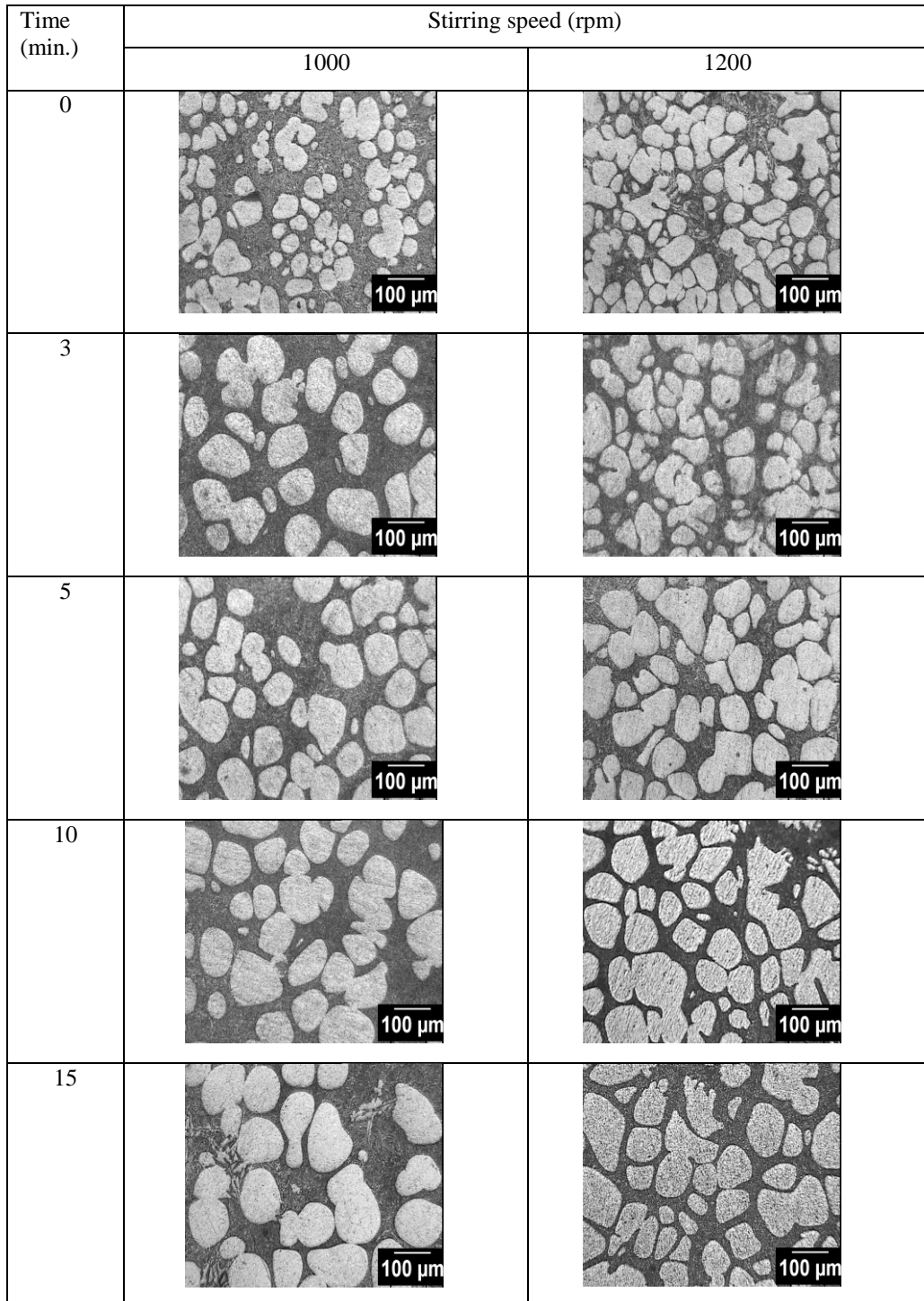


**Fig. 3** Microstructure of RSF processed A356 alloy at different rpm with different holding times

The average grain sizes in all quenched samples at varying stirring speed and holding time are shown in Fig. 4. The results showed that as the stirring speed increased the globularity of the primary  $\alpha$ -Al phase increased and as the holding time increased the average grain size of primary  $\alpha$ -Al phase also increased. Various mechanisms to explain microstructure evolution during coarsening are as given below:

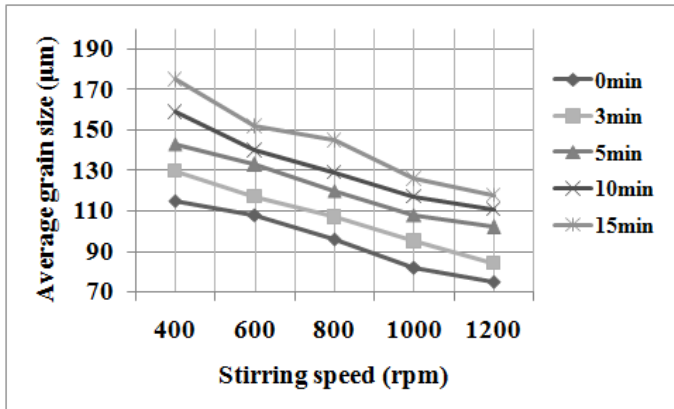


Fig. 4 Variation in the average grain size of A356 alloy with varying stirring speed and holding time

#### Diffusive- LSW theory

In this section, an attempt to find out the average grain size of primary  $\alpha$ -Al phase at different holding time with the help of Ostwald ripening mechanism was carried out. The driving force for Ostwald ripening is the reduction in total interfacial energy. On isothermal holding the microstructure evolution by coarsening and diffusion from high curvature, interface to lower curvature interface takes place [11]. The rate equation can be given as

$$D_M^3 - D_0^3 = K_{fs} K_{LSW} (t - t_0) \quad (1)$$

Where  $D_M$  = the mean grain diameter after time  $t$ ,  $D_0$  = the initial mean grain diameter at time  $t_0$ ,  $K_{fs}$  = the solid fraction coefficient and  $K_{LSW}$  = the growth constant for pure diffusive mass transport [12]. The theoretical value of coarsening rate constant  $K_{cal}$  ( $= K_{fs} \times K_{LSW}$ ) in eq. (1) can be calculated by using the given parameters [13].  $K_{cal}$  for the present case was about  $0.551 \mu\text{m}^3/\text{s}$  using the well-known data for Al-Si alloys. The experimental values of  $K$  obtained from Fig. 5 vary in the range of 949 to  $4678 \mu\text{m}^3/\text{s}$ , which was much higher than the calculated one.

Other investigators [14-16] observed higher coarsening rate in semi-solid processing experiment. Jain et al. [14] in RSF process for 15% solid fraction obtained the experimental value of the coarsening rate constant about  $322 \mu\text{m}^3/\text{s}$ . Kaufmann et al. [15] attained the coarsening rate of 166 and  $430 \mu\text{m}^3/\text{s}$  for the new rheocasting and conventional thixocasting processes, respectively. Zoqui et al. [16] investigated electromagnetic stirring rheocasting process and obtained coarsening rate constants about 1043 and  $3099 \mu\text{m}^3/\text{s}$ . Therefore, the competitive growth of particles related to diffusive Ostwald ripening could not be the only coarsening mechanism. Another phenomenon like convective coarsening and coalescence also contributed to the coarsening in the average grain size of primary  $\alpha$ -Al phase.

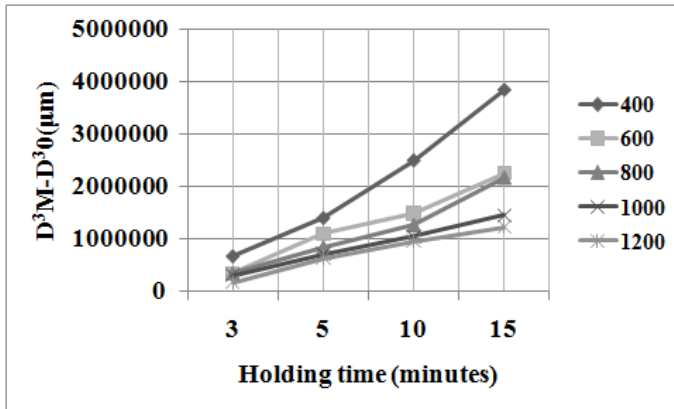


Fig. 5 Variation of a cube of mean particle size with holding time

### Coarsening due to convective mass flow

A theory based on the coarsening due to convective mass flow can be given as

$$D^2 - D_0^2 = AK_{LSW} \frac{(1-f_s)^{2/3}}{f_s} \omega^{1/3} t \quad (2.)$$

Where  $\omega$ = rotation frequency,  $A$ = constant including the diffusion coefficient,  $f_s$ = solid fraction,  $t$ =time [25]. From above eq.2, it is cleared that grain size depends on the square root of time. In the present study comparison between the theoretically and experimental value of coarsening rate constant  $K$  was carried out. The theoretical calculation of  $K$  was carried out using the given parameter [13]. The average calculated value of coarsening rate constant due to convective mass flow  $K_{cal}$  for present investigation was about  $\sim 3451 \mu\text{m}^2/\text{sec}$ , and experimental  $K$  values obtained from Fig.6 varied in the range 8 to  $20 \mu\text{m}^2/\text{sec}$ . So it is cleared that  $K_{cal}$  is greater than  $K_{experis}$  which is just reverse of diffusive-LSW theory.

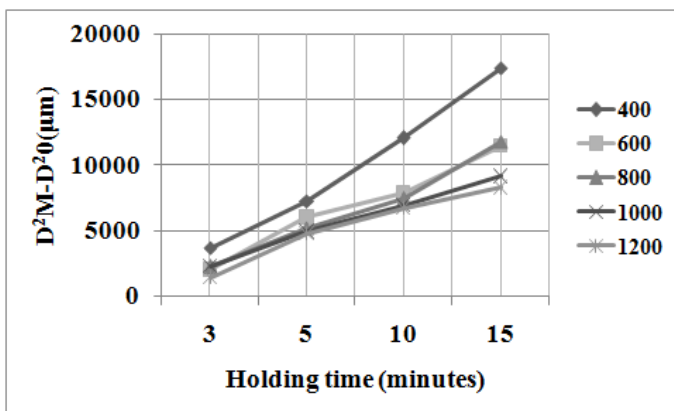


Fig. 6 Variation of the square of mean particle size with holding time

### Analysis of coalescence by shear flow

Since coarsening due to both diffusive-LSW theory and convective mass flow were unable to describe the morphological changed in RSF-processed alloys so it might be suitable to take into

account coalescence phenomena. Due to stirring the shear force led to coalescence of the fragmented and partially melted dendrites in the melt. Such a coalescence process formed the aggregates of large particle size. However, pure collisions could not describe the morphological changes. The theoretical observations by Takajo et al. [17] showed that a combination of Ostwald ripening and coalescence with a size independent collision rate leads to the well-known Ostwald ripening law (cube root growth of the average particle size), but the rate of coarsening kinetics depends on the collision rate (which would here be proportional to the stirring frequency). This model described just the opposite of what was observed: the larger the stirring frequency and thus collision rate, the smaller the overall growth rate [Fig. 5 and Fig. 6].

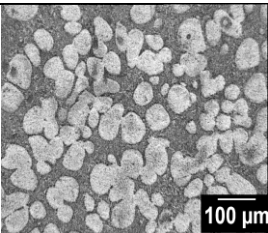
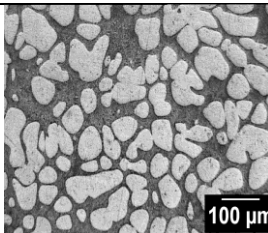
Therefore, aggregation and coalescence phenomena, as well as pure diffusive Ostwald ripening or convective-diffusive Ostwald ripening alone and a combination of Ostwald ripening and coalescence can not describe the change in morphology of primary  $\alpha$ -Al phase (as in Fig. 5 and Fig. 6). Before proceeding let us summarize the significant experimental findings: The average grain size of primary  $\alpha$ -Al phase decreased as the stirring speed increased for all isothermal holding times. The average grain size of primary  $\alpha$ -Al phase increased with holding time, but the rate of coarsening kinetics decreased as the stirring speed increased.

There was a possibility leading to enhanced coarsening rate constants. Shearing and stirring induced turbulence flows, which was complicated by the existence of particles dispersed in the fluid matrix. Generally, in turbulent flow mass transport could not be described by classical diffusion, but the presence of turbulent eddies has to be taken into account flow are accompanied, leading to so-called turbulent diffusion [8]. Turbulent diffusion was much faster than molecular diffusion. The random motion of the fluid was responsible for mixing, with a so-called eddy diffusion coefficient which relies on the properties of the fluid flow, the fluid velocity the size scale of the problem under question [18].

### 3.3 Coarsening kinetics: with the use of baffles

The micrographs show in Fig. 3 illustrated that the stirring speed of 1000 rpm is optimum interms of average grain size and shape factor. Therefore, the experimentation to study about the coarsening kinetics with the use of baffle was carried out at the stirring speed of 1000 rpm with different holding times. Fig. 7 showed the microstructures of the A356 alloy without and with baffle sheared at 1000 rpm with different holding time.

The microstructures prepared with baffle exhibited similar trend for coarsening kinetics as showed in Fig. 3. The microstructures observations showed that the sample prepared with baffle at different holding time comprised fine and more globular primary  $\alpha$ -Al grain morphology than the sample processed without a baffle having same holding time. This change caused the melt to accelerate along the crucible wall and producing the finer and more spherical structure. The mechanism of "nucleation and separation from the wall" has been proposed to justify structural changes with the use of a baffle [19].

Time (min)	Stirring speed (1000rpm)	
	Without Baffle	With Baffle
0		



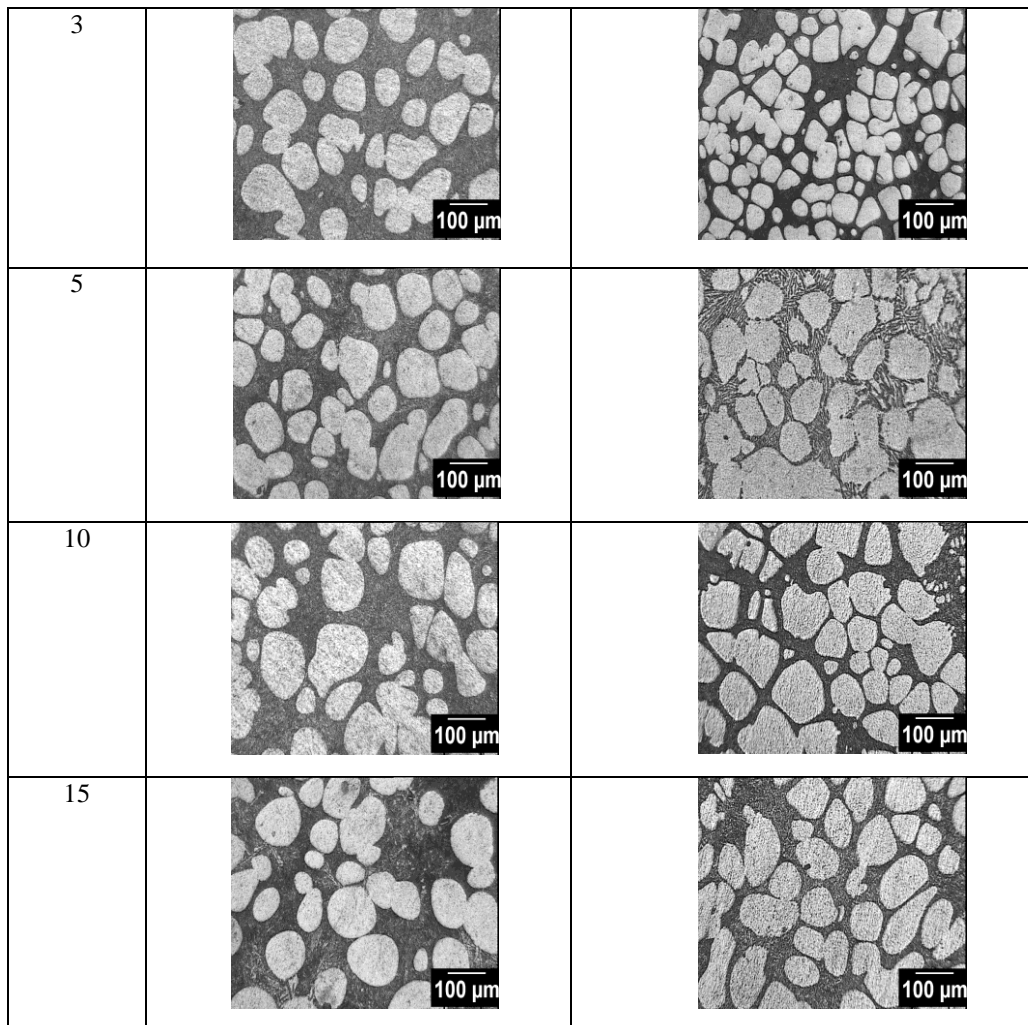


**Fig. 7** Microstructure of RSF processed A356 alloy (a) without and (b) with baffle sheared at 1000rpm but with different holding times

#### 4 Conclusions

RSF process exhibited several potential advantages: (i) components are free from shrinkage porosity and gas porosity, (ii) reduced macro-segregation and hot tearing tendency, (iii) modification of dendritic structure into globular structure, (iv) good heat treatability and mechanical properties, (v) weight saving and near net shape, (vi) high Productivity and increased die life. The average grain size of primary  $\alpha$ -Al phase increased with holding time, but the rate of coarsening kinetics decreased as the stirring speed increased. There was a contribution of diffusive LSW and convective mass flow in the morphological changes during RSF process. However, both were unable to satisfy the explanation fully. Therefore, the coalescence phenomena were also considered. In coalescence process, the small particles combined and formed the aggregates of large particles. The use of baffles comprised a fine and more globular morphology of primary  $\alpha$ -Al and reduced aspiration effect than in samples without the baffle.

## References

- [1] D. B. Spencer, R. Mehrabian, M. C. Flemings: Patent 6, International Material Review, 1972, p. 1932-1935, DOI: 10.1007/BF02642580
- [2] Z. Zhao, Q. Chen, H. Chao, S. Huang: Microstructural evolution and tensile mechanical properties of thixoforged ZK60-Y magnesium alloys produced by two different routes. *Journal of Materials and Design*, Vol. 3, 2010, p. 1906–1916, DOI:10.1016/j.matdes.2009.10.056
- [3] Y. Birol: A357 thixoforming feedstock produced by cooling slope casting, *Journal of Materials Processing Technology*, Vol. 186, 2007, p. 94–101, DOI:10.1016/j.jmatprotec.2006.12.021
- [4] O. Lashkari, R. Ghomashchi: Evolution of primary  $\alpha$ -Al particles during isothermal transformation of rheocast semi solid metal billets of A356 Al–Si alloy, *Canadian Metallurgical Quarterly*, Vol.53, 2014, No. 1, p. 47-54, DOI: 10.1179/1879139513Y.0000000094
- [5] H. V. Atkinson, D. Liu: Coarsening rate of microstructure in semi-solid aluminium alloys *Transactions of Non ferrous Metals Society of China*, Vol. 20, 2010, p. 1672–1676, DOI: 10.1016/S1003-6326(09)60356-3
- [6] N. Haghdad, A. Z. Hanzaki, S. H. Manesh, H. R. Abedi, S. B. H. Irani: The semi-solid microstructural evolution of a severely deformed A356 aluminum alloy, *Materials and Design*, Vol. 49, 2013, p. 878–887, DOI: 10.1016/j.matdes.2013.02.051
- [7] P. J. W. Roberts, D. R. Webster: *Turbulent Diffusion in Environmental Fluid Mechanics Theories and Application*, ASCE, Reston, USA, 2002, p. 1-42, ISBN:0784406294
- [8] S. Ji, Z. Fan: Solidification behavior of Sn-15Pb alloy under a high stirring speed and high intensity of turbulence during semi-solid processing, *Metallurgical and Materials Transactions A*, Vol. 33, 2002, p. 1-12, ISSN: 1073-5623
- [9] ASTM International test standards E 112-12 table 4 macroscopic grain size relationships computed for uniform, randomly oriented, equiaxed grains
- [10] Michel Perez: *Scripta Materialia*, Vol. 52, 2005, p. 709-712, DOI: 10.1016/j.scriptamat.2004.12.026
- [11] S. Terzi, L. Salvo, M. Suery, A. K. Dahle: *Transactions of Indian Institute of Metals*, Vol. 62, 2009, p. 447-449, DOI: 10.1007/s12666-009-0060-7
- [12] P. W. Voorhees, L. Ratke: *Growth and coarsening*, Berlin, Springer, 2002, ISBN: 978-3-662-04884-9
- [13] O. Granath, M. Wessén, H. Cao: *Influence of holding time on particle size of an A356 alloy using the new Rapid Slurry Forming process*, Proc. High Tech Die Casting, AIM, Vicenza, Italy, 2006
- [14] A. Jain, L. Ratke, A. Sharma: *Transactions of Indian Institute of Metals*, Vol. 65, 2012, No. 6, p. 545-551, DOI: 10.1007/s12666-012-0179-9
- [15] H. Kaufmann, H. Wabusseg, P.J. Uggowitzer: *Metallurgical and processing aspects of the NRC semi-solid casting technology*, *Aluminium*, Vol. 76, 2000, No. 1-2, p. 70-75
- [16] E. J. Zoqui, M. T. Shehata, M. Paes, V. Kao, E. E. Sadiqi: *Materials Science and Engineering A*, Vol. 325, 2002, p. 38-53, DOI: 10.1590/S1516-14392010000300006
- [17] S. Takajo, W.A. Kaysser, G. Petzow: *Acta Metallurgica*. Vol. 32, 1984, p. 107-113, DOI: 10.1016/0001-6160(84)90207-4
- [18] M. Reisi, B. Niroumand: *Journal of Alloy and Compound*, Vol. 470, 2009, p. 413–419, DOI: 10.1016/j.jallcom.2008.02.104
- [19] P. Melali, P. Ashtijoo, B. Niroumand: *Metallurgical and Materials Engineering A*, Vol. 21, 2015, No. 1, p. 35-43, DOI: 669.715`721.017.16